

Joint Task Offloading and Resource Allocation for Mobile-Edge Computing Enable Vehicular Networks

Abstract—In order to support delay-sensitive applications of vehicle equipment (V-UE) in the Internet-of-Vehicles (IoV) systems, it is necessary to allow V-UEs to offload their computationally intensive applications to a cloud or edge computing server. Where the uplink channel is reused by multiple vehicles. For the current Mobile-Edge computing enable vehicular networks, interference in the dense vehicle arena often leads to acutely poor communication quality. In addition, a vehicles mobility leads to an uncertain channel state and further affects the stability of communication. The resulting optimization problem corresponds to nonconvex fractional programming, and the block coordinate descent (BCD) algorithm and the successive convex approximation (SCA) technique is proposed to solve it. Furthermore, we decompose the problem into two subproblems for distributed and parallel problem-solving. Numerical simulations are performed to evaluate the algorithm performances, and the results indicate that the proposed algorithm is effective in high mobility under uncertain channel MEC-enable vehicular network environments.

Index Terms—Internet of Vehicle (IOV), Robust Power Control, Edge Computing, Computation Offloading,

I. INTRODUCTION

Urban traffic congestion is becoming more and more serious, traffic accidents are becoming more frequent, and many environmental and energy problems are also caused. Vehicular networks are envisioned to deliver data transmission services ubiquitously, especially in the upcoming autonomous driving era. Accordingly, the high data traffic load poses a heavy burden to the terrestrial network infrastructure. The vehicle speed is fast and the network topology constantly changes under the Vehicle-To-Infrastructure (V2I) environment. The transmission of low delay is also required in intelligent driving tasks, then the data can be transmitted through V2I to complete the intelligent driving task, the vehicle can communicate with the base station (BS) directly or the relay vehicle can help to forward the data.

Considering the rich computing resources provided by the Internet, cloud-based in-car networks have been proposed to address the explosive growth of computing task requirements of vehicles. Traditional cloud computing can no longer meet the stringent low latency requirement of smart driving. Emerging computing mode represented by MEC is rising rapidly [1]. Roadside units (RSUs), which have strong computing capability and are close to vehicle nodes, have been widely used to process delay and computation-intensive tasks of vehicle nodes. Edge computing, which is an information hinge for vehicles and roadside units, can enhance the level of vehicle intelligence in the scene of vehicle-road synergy sensing [2]. Therefore, multiaccess edge computing (MEC) or formerly mobile-edge computing, as new architecture and key technology for the emerging 5G networks, has been proposed

to address the V2I problem [3]. Different from traditional mobile cloud computing (MCC), MEC migrates remote cloud computing resources to the edge of the network to curtail the end-to-end transmission delay of data and to free the computing and storage pressure of vehicles or roadside units [4]. Our objective is to design a comprehensive solution for joint task offloading and resource allocation in a multi-server MEC-enable vehicular network. Specifically, we consider a multi-cell ultra-dense network where each BS is equipped with a MEC server to provide computation offloading services to the mobile vehicles.

A. Related Works

Recently, some works have been devoted to solving problems of computation offloading of mobile devices in MEC or MCC-enable vehicle network architectures. Several works have focused on exploiting the benefits of computation offloading in MEC network [24]. Note that similar problems have been investigated in [5], the horizontal and vertical cooperations between MEC cloud servers are utilized for balancing the workload distribution in dynamic vehicular environment.

Some papers investigated the computation offloading of mobile terminals in single-user scenarios. Aliyu et al. [6] proposed a systematic review of MCC energy-aware issues and grouped some research works on battery energy in MCC into dynamic and nondynamic energy-aware task offloading [5]. Investigate the service scenario of cooperative computation offloading in MEC-assisted service architecture, where multiple MEC servers and remote cloud offload computation-intensive tasks in a collaborative way [1], propose a hybrid transmission and reputation management strategy to accommodate the fast-changing IOV topology and to meet the low latency requirements of intelligent driving tasks. In the V2I networks, the authorized vehicular users with spectrum resources can directly communicate to the RSU. However, the scarce spectrum resources appear inadequate in high-density vehicular networks [7]. To realize more V2X communication under the limited spectrum resources, Chen et al. [8] proposed a Device-to-Device (D2D) crowd framework where a massive crowd of devices at the network edge leverage network-assisted D2D collaboration for computation and communication resource sharing. D2D connects two geographically close devices to achieve low latency communication. D2D can improve spectrum efficiency, reduce cellular network pressure and optimize network performance [9]. Zhou et al. [10] investigated dynamic sharing of the 5G spectrum and proposed a sharing architecture of DSRC and the 5G spectrum for immersive experience-driven vehicular communications. Tran et al. [11] design a holistic solution for joint task offloading and resource

allocation in a multi-server MEC-assisted network. As the vehicles transmitting to the same BS use different sub-bands, the up-link intra-cell interference is well mitigated. It can be seen effective channel reusing is crucial [12], [13] studies resource allocation problems under the one-to-one reusing mode, but the spectrum efficiency of the whole system is low. In order to address the defects of one to one reusing mode, the authors introduce a many-to-one reusing mode where the spectrum utilization is well improved [14].

The moving vehicles, can communicate with different MEC servers in different time slots, and each MEC can only connect with vehicles within its coverage. For the high-speed V2I communication, the generated Doppler effect has a significant influence on the small-scale fading of CSI and thereby causes the fast channel variations. So the temporal correlation coefficient $\rho(T_s)$ is a function of the speed ν and decreases as ν increases, the average sum-rate degenerates as ν grows larger, which means that a larger speed probably endows the acquisition of real-time CSI with more difficulty [15]. In other words, the CSIs used are outdated. Therein, the Bernstein approximation method has commonly been used to deal with this difficult handling non-convex problem [16]. To deal with the interference constraint, the probability constraint is constructed to depress the uncertain co-channel interference. And the Bernstein approximation method is used to transform it into a solvable closed form. To deal with the outage probability constraint, we assume the CSIs are obtained through channel estimation [17]. Therefore, the outage constraint is transformed according to the Bernstein-type inequality to make it a deterministic optimization problem. Based on the characteristics of our constraints, Bernstein method is also used in this paper.

Some papers focused on the problem of computation offloading in the multiple users scenario. Tan and Hu [18] designed a joint communication, caching and computing problem for achieving the operational excellence and the cost efficiency of the vehicular networks. [4] formulated the problem as a generalized NE problem and presented a game theory algorithm to analysis the equilibrium problem. It is assumed in [4] that the vehicles use a constant transmit power while our approach optimizes vehicles transmit power. However, it seems like a new problem because the objective function is difficult to handle. Nemirovski and Shapiro have proposed a convex approximation approach in [19] that can solve it. In summary, most of the existing works did not consider a holistic approach that jointly power control and the computing resource allocation in a multi-vehicles, multi-MEC system as considered in this paper.

B. Challenges and Contributions

Generally, for the low-speed V2X communication case, the Doppler effect is not noticeable, thereby being ignored, but the high mobility of vehicles poses a challenge to V2X communication. It is analyzed that the original stochastic optimization problem with two variables can be transformed into a deterministic non-convex optimization problem. It is likely to bring a new difficulty.

The main contributions are summarized as follows:

- The Doppler effect in the process of high-speed movement of vehicles will affect the communication quality between vehicles and roadside units, different from previous studies, this paper considers the mobility of vehicles in the research of the edge computing system of the Internet of Vehicles, and verifies the adverse effects of vehicle mobility through comparative simulation.
- We propose an efficient hybrid transmission task scheduling strategy. The transmission mode is predicted, and the task is scheduled according to the vehicle context. V2V transmission is adopted to minimize the delay when the task-initiating vehicle cannot complete the task independently.
- Considering the channel uncertainty caused by the high-speed movement of vehicles in the scenario of the Internet of Vehicles, the first-order Markov process is introduced. A reasonable and feasible IoV network scenario is constructed to more realistically describe the dynamic characteristics of the Internet of Vehicles. The Bernstein approximation method previously used in interference constraints is improved and generalized, and it is applied to the matrix form of interruption probability to deal with non-convex signal-to-interference noise ratio constraints in large-scale dynamic vehicle network environments to ensure the quality of network communication services.

The remainder of this article is organized as follows: the model of computation offloading in MEC-assisted vehicular networks is established defines in Section II, In Section III, the probability constraints and the objective function of the primal problem are formulated, and the optimization is proposed. In Section IV, simulation results and performance analysis are presented. Finally, we draw a conclusion in Section V.

II. SYSTEM MODEL

In this paper, we consider a IoV edge computing network, consisting of a cloud computing layer, MEC layer, as shown in Fig. 1. For MEC layer, which has moderate computation capacity and deploys close to networks, can be used to assist the vehicles. Cloud computing layer, can be used to process the large-scale, delay-insensitive data that MEC layer can not process. [20] Numerous vehicle-to-RSU (V2I) cells underlay a cell. In which each RSU is equipped with a MEC server to provide computation offloading services to the vehicles. To avoid inter-cell interference, the time division multiple access (TDMA) communication technology is adopted. Time resource is divided into multi-frames, and each frame is divided into several time slots. Different vehicles access its time slots when they communicate with the RSU, and signal transmission in different time slots will produce no interference [10]. We denote the set of vehicles and MEC servers in the mobile system as $V = \{1, 2, \dots, V\}$ and $M = \{1, 2, \dots, M\}$, respectively. Some notations are given in Table I.

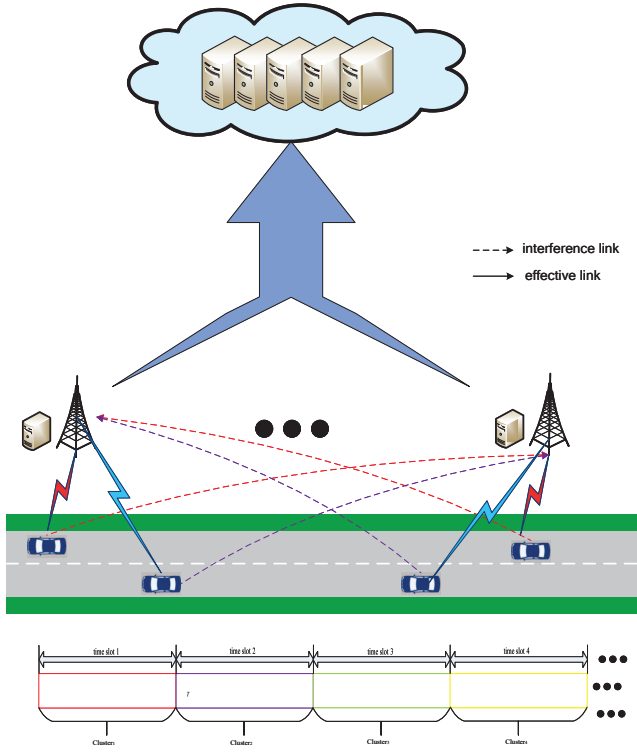


Fig. 1: System model.

TABLE I: Notations

$\Pr\{\cdot\}$	Probability function.
\mathbb{R}^k	Set of k -dimensional real vectors.
\mathcal{M}	Index set of vehicles over a time slot $\mathcal{M}=\{1, 2, \dots, M\}$.
\mathcal{V}	Index set of all active vehicles $\mathcal{V}=\{1, 2, \dots, V\}$.

A. Communication Model

Different from the traditional cellular communication, Due to the fast mobility of vehicles, their CSIs are hard to be estimated precisely. In particular, RSU can only achieve the accurate knowledge of large-scale fading L^2 of vehicular to RSU links while the small-scale fading h is greatly influenced by the fast channel variations caused by the Doppler effect. We assume the CSIs are obtained through channel estimation [17]. Therefore, we model the small-scale fading channel estimation of h by using the first-order Gauss-Markov process [21] in each transmission time interval (TTI) as follows,

$$h = \xi \tilde{h} + \sqrt{1 - \xi^2} \zeta, \quad (1)$$

We assume that the estimated channel gain \tilde{h} denotes the estimate of h and \tilde{h}^2 is exponentially distributed with unit mean [22]. Furthermore, $\xi \in (0, 1)$ represents the correlation coefficient over $v \rightarrow m$ link, and ζ stands for the channel gain and follows a complex Gaussian distribution $\zeta \sim CN(0, \delta^2)$ and independent and uncorrelated of \tilde{h} . The coefficient ($0 < \zeta < 1$) quantifies the channel correlation between the two consecutive time slots and we assume that time correlation coefficient ζ is same for all VUEs. According

to the Jakes statistical model for the fading channel [21], ζ is given as $\zeta = J_0(2\pi f_{max} T_s)$, where J_0 is the zero-order Bessel function of the first kind. $f_{max} = \bar{v} f_c / c$ is the maximum Doppler frequency, where \bar{v} indicates the vehicle speed, f_c indicates the carrier frequency at 5.9 Ghz, and $c = 3 \times 10^8 m/s$ is a period feedback latency. erally, both transmitter vehicles and RSU can know the accurate ζ .

Based on the aforementioned discussion, the mobile V2I channel power gain of the effective links and interference links in k_{th} time slot from i_{th} transmitter to j_{th} receiver can be expressed as a shared expression:

$$G_{i,j}^k = \hat{g}_{i,j}^k + \tilde{g}_{i,j}^k, \quad (2)$$

Where $\hat{g}_{i,j}^k = L_{i,j}^2 \tilde{h}_{i,j}^2 \xi_{i,j}^2$, $\tilde{g}_{i,j}^k = L_{i,j}^2 (1 - \xi_{i,j}^2) \zeta_{i,j}^2$, and $L_{i,j}^k$ denotes the k th time slot large-scale fading effects including shadow-fading and path loss from i_{th} transmitter to j_{th} receiver on the road section. Moreover, $\hat{g}_{i,j}^k$ is an observed value. $\tilde{g}_{i,j}^k$ denotes an exponential random variable with parameter, $E\left(\frac{1}{L_{i,j}^k \sqrt{1 - \xi_{i,j}^2}}\right)$.

To improve the spectrum utilization and realize multi-vehicles joint communication, V2I communications reuse the same uplink channel. In this case, the Signal-to-Interference-plus-Noise Ratio (SINR) from vehicle i to RSU can be formulated as,

$$\gamma_i^v = \frac{p_i g_{i,j}}{\sum_{j=1, j \neq i}^M p_j g_{j,i} + \sigma^2} \quad (3)$$

Where p_j denotes the transmit power of the j_{th} vehicles, where σ^2 is the background noise. Therefore, the deterministic equivalent transmission rate of VUEs calculated by Shannons theorem is,

$$R_i(P) = \log_2 \left(1 + \frac{p_i g_{i,j}}{\sum_{j=1, j \neq i}^M p_j g_{j,i} + \sigma^2} \right) \quad (4)$$

Hence, the transmission time of vehicle i when sending its task input $d_{i,up}$ in the uplink can be calculated as,

$$t_{i,up} = \frac{d_{i,up}}{R_i(P)} \quad (5)$$

Where W is the bandwidth of the reused channel. Therefore, the upload time of each V2I link can be formulated as,

$$t_{i,up} = \frac{d_{i,up}}{W \log_2 \left(1 + \frac{p_i g_{i,j}}{\sum_{j=1, j \neq i}^M p_j g_{j,i} + \sigma^2} \right)} \quad (6)$$

And $d_{i,up}$ is the amount of input data including system settings, program codes, and input parameters, which is necessary to transfer the program execution.

Communication delay is another significant index that affects the performance of wireless networks. The packets to V2I receivers must be in the queue before they transmit at the speed of R_i . It is assumed that the process of a packet arriving at the i_{th} V2I receiver is a Poisson process with parameter k_i , and the length of the data packet obeys the exponential distribution of parameter τ_i . We develop the M/M/1 model

instructions the relationship between the expected delay and transmission rate of the i_{th} V2I links can be expressed as,

$$D_i = \frac{1}{\tau_i R_i - k_i} \quad (7)$$

B. Vehicle Computing Model

We consider that each vehicle $v \in V$ has one different computation task at a time. denoted as c_v [cycles] specifies the workload, i.e. the amount of computation to accomplish the task, that is atomic and cannot be divided into subtasks. The values of c_v can be obtained through carefully profiling of the task execution [23]. Each task should be offloaded to the MEC server and then transmission to the cloud server. By offloading the computation task to the MEC server, the vehicles would get more computing resources, however, it would consume additional time for sending the task input in the uplink.

The MEC server at each RSU is able to provide computation offloading service to a vehicle at a time slot. The computing resources are quantified by the fixed rate \bar{f} , expressed in terms of number of CPU cycles/s. the vehicle i_{th} uploads the input data of task to the nearest RSU, the RSU process the small-scale, delay-sensitive data first, then the RSU forward the remaining data to the remote cloud server, the cloud is able to provide computation offloading service to multiple RSU concurrently. The computing resources made available by cloud to be shared among the associating users are quantified by the computational rate f_i , it is still expressed in terms of number of CPU cycles/s. Thus, the latency for computing offloading can be written as,

$$t_{i,exe} = \frac{c_{i,e}}{\bar{f} + f_i} \quad (8)$$

C. Problem Definition

Given the computing resource allocation f_i , the total delay experienced by vehicle i when offloading its task is given by,

$$t_i = \frac{c_{i,e}}{\bar{f} + f_i} + T_c \quad (9)$$

The transmission latency between RSU and cloud server is defined as T_c , usually it is set to a fix value [17], so the relative improvement in task completion time is characterized by,

$$U_{i,exe} = \frac{t_{max} - t_{i,exe}}{t_{max}} \quad (10)$$

Where t_{max} is the maximum tolerable threshold of the task completion time. If a task can be completed ahead of deadline t_{max} , the vehicle can get a higher utility, otherwise, it will produce the corresponding loss. Therefore, we define the offloading utility of vehicle u as,

$$\frac{U_{i,exe}}{t_{i,up}} \quad (11)$$

denote offloading time cost utilities at a unit.

The joint task offloading and resource allocation will be formulated as an optimization problem in this section. And the goal is to obtain the minimum total system cost composed of latency and transmission rate for all vehicles in the networks. For a given uplink power allocation \mathbf{p} , and computing resource

allocation \mathbf{f} , we define the system utility as the weighted-sum of all the vehicles offloading utilities,

$$U = \max \sum_{i=1}^M \frac{U_{i,exe}}{t_{i,up}} \quad (12)$$

This utility means getting a more enormous execution time utility with a minor upload time cost. We now formulate the Joint Resource Allocation and Task Offloading Problem as a system utility maximization problem, i.e. The robust optimization problem is formulated as follows:

$$\mathbf{P} : U = \max \sum_{i=1}^M \frac{U_{i,exe}}{t_{i,up}} \quad (13a)$$

$$s.t. \begin{cases} Pr \{ \gamma_i \geq \gamma_{th} \} \geq 1 - \varepsilon_1, \\ Pr \left\{ \frac{1}{\tau_i R_i - k_i} + \frac{c_{i,e}}{\bar{f} + f_i} \leq D_{max} \right\} \geq 1 - \varepsilon_2, \\ \sum_{i=1}^N f_i \leq f_{total}, \\ 0 \leq p_i \leq p_{max} \end{cases} \quad (13b)$$

$$(13c)$$

$$(13d)$$

$$(13e)$$

Where U denotes the network utility, the constraints in the formulation above can be explained as follows: Constraints (13a) is used to guarantee the QoS requirements of VUEs, however, due to Large amount of computation caused by time varying network topologies, the real-time SINR is hard to obtain in vehicular communication scenario, and it can be replaced with the long-term SINR since the CSI feedback time interval is very small. γ_i denotes the average SINR of the i_{th} V2I link when a small CSI feedback time interval is used, in order to ensure that the task is successfully offloaded to the RSU, the SINR should be guaranteed to be no less than the SINR threshold [24]. γ_{th} is the SINR threshold for successful detecting the V2I communication. $p_r \{ \cdot \}$ defines the probability of the input. In this case, we introduce the outage probability constraint (13a) to guarantee the reliability of vehicular links [25]. D_{max} is the delay bound of the i_{th} V2I link in the process of data transmission. $\varepsilon_1, \varepsilon_2$ are the outage probability thresholds of SINR and delay constraint respectively, where $\varepsilon_1, \varepsilon_2 \in (0, 1)$. constraints (13c) state that each MEC server must allocate a positive computing resource to each user associated with it and that the total computing resources allocated to all the associated users must not exceed the servers computing capacity, in another word, the number of applications served by a particular edge cloud should be within its capacity. (13b) denote the total latency of communication and computing should be guaranteed to be no less than the time threshold, p_{max} is the maximum transmit power of the transmit vehicle in vehicle communication network, and the transmit power is greater than zero in (13d).

III. PROBLEM SOLUTIONS

In this section, we proposed a BCD-based algorithm to solve the problem (13). The BCD method enables the complex original problem to be decomposed into a succession of simpler subproblems [26]. Motivated by this fact, all variables are divided into two blocks and optimized alternatively.

By fixing \mathbf{f} , the problem (13) can be transformed into the following problem.

$$\mathbf{P1} : U = \max \sum_{i=1}^M \frac{U_{i,exe}}{t_{i,up}} \quad (14a)$$

$$s.t. \begin{cases} Pr \{ \gamma_i \geq \gamma_{th} \} \geq 1 - \varepsilon_1 \end{cases} \quad (14b)$$

$$\begin{cases} Pr \left\{ \frac{1}{\tau_i R_i - k_i} + \frac{c_{i,e}}{\bar{f} + f_i} \leq D_{max} \right\} \geq 1 - \varepsilon_2 \\ 0 \leq p_i \leq p_{max} \end{cases} \quad (14c)$$

$$(14d)$$

A. Successive Convex Approximation of the Objective Function

Since the original problem is a non-convex and NP-hard because of the logarithmic function in the objective function, here, the method of successive convex approximation is adopted to relax the original problem and make objective function solvable. We can use the lower bound to approach the original function as follows,

$$\begin{cases} \alpha \ln(z) + \beta \leq \ln(1+z) \\ \alpha = \frac{z_0}{1+z_0} \\ \beta = \ln(1+z_0) - \frac{z_0}{1+z_0} \ln(z_0) \end{cases} \quad (15)$$

Each term of (14) can be represented by $A_k \ln(\gamma_k(e^{\tilde{P}})) + B_k$ through successive convex approximation, where A_k and B_k can be chosen as $A_k = \gamma_i / (1 + \gamma_i)$, $B_k = \ln(1 + \gamma_i) - A_k \ln(\gamma_i)$, $A_k=1$, $B_k=0$, and each term of objective function can be written as follows,

$$\frac{1}{\ln 2} \sum_{i=1}^M \frac{U_{i,exe}}{d_{i,up}} [A_k \ln(\gamma(p)) + B_k] \quad (16)$$

It is still hard to directly calculation because of fractional from of SINR, we use variable substitution, i.e. $\hat{p}_i = \ln p_i$, $p_i = e^{\hat{p}_i}$, then $\hat{p}_i \leq \ln p_{max}$, $\forall 1 \leq i \leq M$

$$U = \max \frac{1}{\ln 2} \sum_{i=1}^M \frac{U_{i,exe}}{d_{i,up}} [A_k \ln(\gamma(e^{\tilde{P}})) + B_k] \quad (17)$$

B. Approximate of the Outage Probability Constraint

It is obvious that the constraint (14a) includes uncertainties and the objective function is a non-convex problem in (14), so the objective function and constraints are difficult to deal with when determining the optimal solutions. It is necessary to design an algorithm with lower complexity to solve the problem. In this paper, For the uncertain channel gain. Considering the fast fading. Two common forms are adopted to describe the uncertainty mentioned above, i.e. the statistical constraints and deterministic constraints. to pursue a simple form of (14a), a matrix form is introduced, the general form the channel gain is described as,

$$Pr \left\{ (G_m)^T e^{\tilde{P}} + \sigma^2 \leq 0 \right\} \geq 1 - \varepsilon_1 \quad (18)$$

Where $\mathbf{G}_m = [G_{1,m}, G_{2,m}, \dots, -\frac{G_{m,m}}{\gamma_{th}}, \dots, G_{M,m}]^T$, Furthermore, the Bernstein method is adopted to approximate the probability constraint with channel uncertainty

Theorem 1: The outage probability of all cochannel V2I links $Pr \{ \gamma_i \leq \gamma_{th} \} \geq 1 - \varepsilon_1$ is reformulated as the separable constraints (14a)

$$\sigma^2 + \sum_{i=1}^M \chi_{i,j} e^{\tilde{P}_i} + \sqrt{2 \ln \left(\frac{1}{\varepsilon_1} \right)} \left(\sum_{m=1}^M (\sigma_{i,j} \beta_{i,j} p_i)^2 \right)^{\frac{1}{2}} \leq 0, \quad (19)$$

Where $\chi_{i,j} = \mu_{i,j}^+ \alpha_{i,j} + \beta_{i,j} + g_{i,j}$, these parameters (i.e. $\sigma_{i,j}$ and $\alpha_{i,j}$) are deduced to be positive in [27]. Suppose that the truncated distributions of $G_{i,j}$ have bounded supports $[\tilde{g}_{i,j}^k + \alpha_{i,j}, \tilde{g}_{i,j}^k + \beta_{i,j}]$, $\tilde{g}_{i,j}^k$ is an estimate of $G_{i,j}$, Introduce constants $\alpha_{i,j} = \frac{1}{2}(b_{i,j} - a_{i,j})$, $\beta_{i,j} = \frac{1}{2}(b_{i,j} + a_{i,j})$ to normalize the supports to $[-1, 1]$ as follows,

$$\xi_{i,j} = \frac{G_{i,j} - \tilde{g}_{i,j}^k - \beta_{i,j}}{\alpha_{i,j}} \in [-1, 1], \quad (20)$$

In the last term of (19), the variables p are coupled nonlinearly. Hence, directly finding an acceptably good solution to (14a) by the Bernstein method is time consuming when the K increases and the number of vehicles is large. Therefore, it is necessary to Introduced a l_2 -norm approximate problem for any $x \in \mathbb{R}^k$. Hence, the last term in (19) containing l_2 -norm of the vector is further approximated by $\|x\|_1 \leq \|x\|_2$. Based on these, the constraint in (14a) is further formulated as fellow with lower complexity and higher reliability,

$$\sigma^2 + \sum_{i=1}^M \chi_{i,j} e^{\tilde{P}_i} + \sqrt{2 \ln \left(\frac{1}{\varepsilon_1} \right)} \sum_{i=1}^M |\sigma_{i,j} \beta_{i,j}| e^{\tilde{P}_i} \leq 0 \quad (21)$$

To pursue a simple form of (21), we define

$$\Pi_i = \sigma^2 + \sqrt{2 \ln \left(\frac{1}{\varepsilon_1} \right)} \sum_{i \neq j} |\sigma_{i,j} \beta_{i,j}| e^{\tilde{P}_i} \quad (22)$$

The constraint (14b) can be handled by an Integral transformation method, According to constraint (14b), where $D_{max} = D_1 + D_2$, $D_1 = \frac{1}{\tau_i R_i - k_i}$, $D_2 = \frac{c_{i,e}}{f_i}$, $X = \tilde{h}^2$ is an exponential random variable with unit mean, i.e., $X \sim \exp(1)$, we can get the feasible power region of the communication delay probability as follows,

$$[\ln(1 - \varepsilon_2) - \hat{g}_{i,j}^k] e^{\tilde{P}_i} + D^* \leq 0 \quad (23)$$

The proof of the feasible region can be found as follow,

Proof: The probability constraint of (14b) can be transformed to the deterministic one according to the following inference

$$\begin{aligned} & Pr \left\{ \frac{1}{\tau_i R_i - k_i} + \frac{c_{i,e}}{f_i} \leq D_{max} \right\} \\ &= Pr \left\{ R_i \geq \frac{1}{R_i(D_{max} - D_2)} + \frac{k_i}{\tau_i} \right\} \\ &\leq 1 - Pr \left\{ p_i \tilde{g}_{i,j}^k \leq (I_{th} + \sigma^2) 2^{\frac{1+k_i(D_{max}-D_2)}{\tau_i(D_{max}-D_2)}} - p_i \hat{g}_{i,j}^k \right\} \\ &= 1 - \int_0^{(I_{th} + \sigma^2) 2^{\frac{1+k_i(D_{max}-D_2)}{\tau_i(D_{max}-D_2)}} - p_i \hat{g}_{i,j}^k} e^{-x} dx \geq 1 - \varepsilon_2 \end{aligned} \quad (24)$$

Then, we have the equivalent result of the inequality function in (24) as

$$[\ln(1 - \varepsilon_2) - \hat{g}_{i,j}^k] e^{\tilde{P}_i} + D^* \leq 0 \quad (25)$$

Where, $D^* = (I_{th} + \sigma^2) 2^{\frac{1+k_i(D_{max}-D_2)}{\tau_i(D_{max}-D_2)}}$ ■

In summary, we can obtain a deterministic optimization problem of robust power allocation by transforming the objective function, outage probability constraints, delay constraints. It is expressed as,

$$\mathbf{P1} : \max_{\mathbf{p}} \frac{1}{\ln 2} \sum_{i=1}^M \frac{U_{i,exe}}{d_{i,up}} \left[A_k \ln(\gamma(e^{\tilde{p}})) + B_k \right] \quad (26a)$$

$$s.t. \begin{cases} \sum_{i=1}^M \chi_{i,j} e^{\tilde{p}_i} + \Pi_i \leq 0 \\ \left[\ln(1 - \varepsilon_2) - \hat{g}_{i,j}^k \right] e^{\tilde{p}_i} + D^* \leq 0 \\ -\infty \leq \tilde{p}_i \leq \ln p_{i,max} \end{cases} \quad (26b)$$

$$s.t. \begin{cases} \left[\ln(1 - \varepsilon_2) - \hat{g}_{i,j}^k \right] e^{\tilde{p}_i} + D^* \leq 0 \\ -\infty \leq \tilde{p}_i \leq \ln p_{i,max} \end{cases} \quad (26c)$$

$$s.t. \begin{cases} \left[\ln(1 - \varepsilon_2) - \hat{g}_{i,j}^k \right] e^{\tilde{p}_i} + D^* \leq 0 \\ -\infty \leq \tilde{p}_i \leq \ln p_{i,max} \end{cases} \quad (26d)$$

C. Optimal Power Control Algorithm

To pursue an iterative algorithm for solving the problem, Lagrange method is used to maximize the lower bound of the original objective under given coefficients X_i and Y_i . It is noted that these two coefficients should be updated to guarantee a monotonic increase in the lower bound performance.

Hence, the Lagrangian function of (26) under fixed coefficients X_i and Y_i can be expressed as,

$$L(\tilde{\mathbf{p}}, \lambda, \mu) = \frac{1}{\ln 2} \sum_{i=1}^M \frac{U_{i,exe}}{d_{i,up}} \left[A_k \ln(\tilde{\gamma}_k(e^{\tilde{\mathbf{p}}})) + B_k \right] \quad (27)$$

$$- \mu_k \left[\left(\ln(1 - \varepsilon_2) - \hat{g}_{i,j}^k \right) e^{\tilde{p}_i} + D^* \right]$$

$$- \lambda_k \left[\sum_{i=1}^M \chi_{i,j} e^{\tilde{p}_i} + \Pi_i \right],$$

Where λ_k and μ_k are the Lagrangian multipliers, and $\lambda_k \geq 0$, $\mu_k \geq 0$.

The power vector \mathbf{p} iteration function is obtained by

$$\frac{\partial L(\mathbf{p}, \lambda, \mu)}{\partial p_i} = A_i - \left[\sum_{j=1, j \neq i}^M \left(A_j \frac{\tilde{\gamma}_j(e^{\tilde{\mathbf{p}}}) \tilde{G}_{k,j}}{e^{\tilde{p}_j} \tilde{G}_{j,j}} \right) \right] \quad (28)$$

$$+ \lambda_i \Pi_i e^{-\tilde{p}_i} + \mu_i \hat{g}_{i,j}^k \Big] e^{\tilde{p}_i} = 0$$

Based on (28), the iteration for the power allocation, can be formulated as,

$$\tilde{p}^{(t+1)} = \left[\ln A_i + \ln \left(\sum_{j=1, j \neq i}^M \left(A_j \frac{\tilde{\gamma}_j(e^{\tilde{\mathbf{p}}}) \tilde{G}_{k,j}}{e^{\tilde{p}_j} \tilde{G}_{j,j}} \right) \right) \right. \\ \left. + \lambda_i \Pi_i e^{-\tilde{p}_i} + \mu_i \hat{g}_{i,j}^k \right]_{-\infty}^{\ln p_{i,max}} \quad (29)$$

The Lagrangian multiplier λ , μ , are updated through the sub-gradient method, which are formulated as,

$$\lambda_i^{(t+1)} = \left[\lambda_i^{(t)} + K_\lambda^{(t)} \left(\sum_{j \neq i}^M \chi_{i,j} e^{\tilde{p}_j} + \Pi_i \right) \right]^+ \quad (30)$$

$$\mu_{i,j}^{(t+1)} = \left[\mu_{i,j}^{(t)} + K_\mu \left(\left(\ln(1 - \varepsilon_2) - \hat{g}_{i,j}^k \right) e^{\tilde{p}_i} + D^* \right) \right]^+ \quad (31)$$

Where K_λ , K_μ denote the step-size, and $K_\lambda \geq 0$, $K_\mu \geq 0$. t denotes the iteration index. $[x]^+ = \max[0, x]$.

D. Computing Resource Allocation

After obtaining \mathbf{p} , the formulated problem with respect \mathbf{f} reformulated by:

$$\mathbf{P2} : \max \sum_{i=1}^N \frac{U_{i,exe}}{t_{i,up}} \quad (32a)$$

$$s.t. \begin{cases} \Pr \{ \gamma_i \leq \gamma_{th} \} \geq 1 - \varepsilon_1 \end{cases} \quad (32b)$$

$$\Pr \left\{ \frac{1}{\tau_i R_i - k_i} + \frac{c_{i,e}}{\bar{f} + f_i} \leq D_{max} \right\} \geq 1 - \varepsilon_2 \quad (32c)$$

$$0 \leq P_i \leq P_{i,max} \quad (32d)$$

Notice that the constraints in (32a) and (32b) are convex, by calculating the second-order derivatives of f_i , the Lagrangian function is constructed to seek the optimal powers. Hence, (32) is a convex optimization problem and can be solved using Karush-Kuhn-Tucker (KKT) conditions. The Lagrangian function of (32) is formulated as,

$$U(\mathbf{f}, \xi, \varphi) = \sum_{i=1}^M \frac{R_i(P)}{\ln 2 * d_{i,up}} \left[1 - \left(\frac{c_{i,e}}{t_{max}(\bar{f} + f_i)} + \frac{T_c}{t_{max}} \right) \right]$$

$$- \xi_k \left(\frac{1}{\tau_i R_i - \lambda_i} + \frac{c_{i,e}}{\bar{f} + f_i} \leq D_{max} \right) - \varphi_k \left[\sum_{i=1}^M f_i - f_{total} \right] \quad (33)$$

Based on (33), the iteration for the computing resource allocation, can be formulated as, In order to prove the concavity of (32), the following research is taken. The first-order derivative of $U(\mathbf{f}, \xi, \varphi)$ with respect to f_i is,

$$\frac{\partial U(\mathbf{f}, \xi, \varphi)}{\partial f_i} = \frac{c_{i,e}}{\ln 2 * d_{i,up} t_{max} (\bar{f} + f_i)^2} = \frac{\Omega_i}{(\bar{f} + f_i)^2} \quad (34)$$

in which, for simplicity

$$\Omega_i = \frac{c_{i,e}}{\ln 2 * d_{i,up} * t_{max}}$$

The second-order derivative of is obtained further as,

$$\frac{\partial^2 U}{\partial f_i^2} = - \frac{2 * \Omega_i}{(\bar{f} + f_i)^3} \leq 0 \quad (35)$$

It is obvious that the second-order derivative of $U(\mathbf{f}, \xi, \varphi)$ with respect to f_i is always less than zero. Therefore, $U(\mathbf{f}, \xi, \varphi)$ is a concave function about f_i . Hence, (32) is a convex optimization problem and can be solved using Karush-Kuhn-Tucker (KKT) conditions.

$$\frac{\partial u(\mathbf{F}, \xi, \varphi)}{\partial f_i} = \frac{\Omega_i R_i(P)}{(\bar{f} + f_i)^2} - \xi_k \frac{c_{i,e}}{(\bar{f} + f_i)^2} - \sum_{i=1}^N \varphi_k = 0 \quad (36)$$

Let

$$\frac{\partial u(\mathbf{F}, \xi, \varphi)}{\partial f_i} = 0$$

the optimal computing resource allocation is:obtained by

$$f_i^* = \sqrt{\frac{\Omega_i R_i(P) - c_{i,e} \xi_k}{\sum_{i=1}^N \varphi_k}} - \bar{f} \quad (37)$$

The iterative expression is as follows,

$$\tilde{f}^{(t+1)} = \left[\sqrt{\frac{\Omega_y R_i(P) - c_{i,e} \xi_k}{\sum_{k=1}^M \varphi_k}} - \bar{f} \right]_0^{f_{total}} \quad (38)$$

The Lagrangian multiplier η , φ , are updated through the sub-gradient method, which are formulated as,

$$\xi_i^{(t+1)} = \left[\xi_i^{(t)} + K_\xi^{(t)} \left(\frac{1}{\tau_i R_i - \lambda_i} + \frac{c_{i,e}}{\bar{f} + f_i} - D_{max} \right) \right]^+ \quad (39)$$

$$\varphi_{i,j}^{(t+1)} = \left[\varphi_{i,j}^{(t)} + K_\varphi \left(\sum_{i=1}^M f_i - f_{total} \right) \right]^+ \quad (40)$$

With the above efforts, we successfully transform the original problem into two convex subproblems. Then, an alternative iterative algorithm which is summarized in Algorithm 1 is proposed to solve them.

Algorithm 1 Joint Robust Power Control Task Offloading Scheduling Algorithm

- 1: **Input:** Set the maximal iterative number \mathcal{T}_{max} , and the iterative index $t = 0$.
 - 2: **repeat**
 - 3: Given feasible points λ, μ, \mathbf{f} .
 - 4: Solve problem P_1 , and obtain the current optimal solution $\tilde{p}^{(t+1)}$.
 - 5: Given feasible points ξ, φ, \mathbf{p} .
 - 6: Solve the problem P_2 , and obtain the current optimal solution $\tilde{f}^{(t+1)}$.
 - 7: **until** synchronously converge to the optimal solutions or $t \geq \mathcal{T}_{max}$
 - 8: **Output:** \mathbf{f}, \mathbf{p} .
-

Remark 1. Algorithm1 contains a loop whose time complexity is described by the maximal loop count, \mathcal{T}_{max} . Since there are V clusters which use their power iterations for power optimization, the computational complexity of the Algorithm1 is $O(V\mathcal{T}_{max})$.

IV. SIMULATION AND PERFORMANCE EVALUATION

In this section, numerical simulations are presented to evaluate the performance of the proposed Algorithm1. A MEC-based vehicular network system which includes five clusters under a certain time slot is selected as our fundamental simulation scenario. The major system parameters are listed in Table II. It is noted that the bandwidth W is set as 10 MHz in the numerical simulations. We assume that both the vehicles and RSUs use a single antenna for uplink transmission and reception, respectively, and the variation of the vehicles speed is negligible within the reference time interval. Unless stated otherwise, the parameter value of γ_{th} is set to 10^{-6} , the outage probability threshold $\varepsilon_1 = \varepsilon_2 = 0.1$.

TABLE II: System parameters

Parameter	Value
Carrier frequency (f_c)	5.9 GHz
Radio Range (R_a)	300 m
CSI feedback period of vehicle (T)	1 ms
Average speed of vehicle	30 m/s
Mean of background noise (σ^2)	-30 dBm
Maximum transmitter power ($p_{i,max}$)	0.05 W
Log-normal shadowing standard deviation	10 dB
Pathloss model	$d^{-\theta}$, d in m
Pathloss exponent (θ)	3

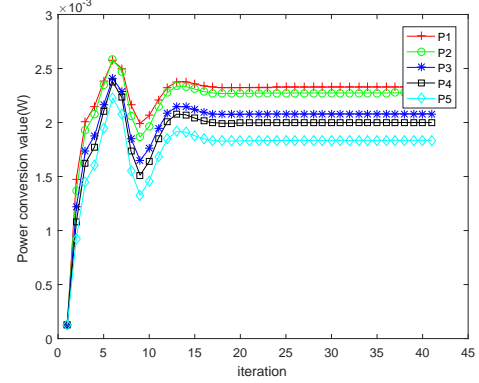


Fig. 2: Power convergence performance.

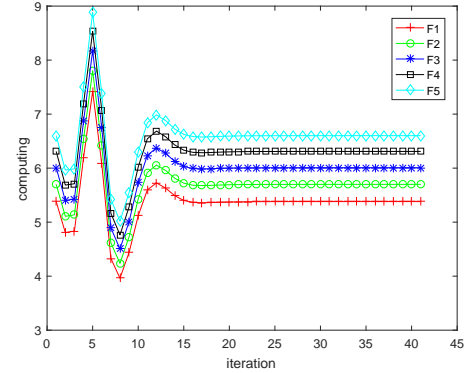


Fig. 3: computing resource which cloud allocation to RSU.

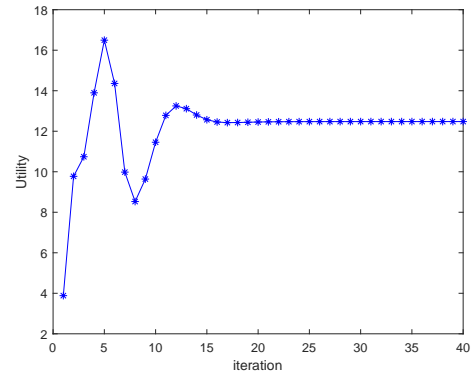


Fig. 4: Comparison of average system utility.

Fig. 1 and Fig. 2 show the power allocation of each vehicle

transmitter and the corresponding computing resource which cloud allocation to RSU in Algorithm1, respectively. It can be seen that the computing resources allocated in the cloud peak at the fifth iteration and begin to decline because of the limitation of total computing resources f_{total} from the cloud. The corresponding power resource allocation also changes due to computing resources allocation under Joint Robust Power Control and Task Offloading Scheduling.

This phenomenon is reasonable due to the definition of U in (12). R_i increases logarithmically as the power vector \mathbf{p} increases, the upload time $t_{i,up}$, as the denominator of U , will decrease with the increase of power vector \mathbf{p} and as the executive utility of the numerator part, $t_{i,exe}$ decreases inversely proportional with the increase of computing power \mathbf{f} , causing the numerator to increase with the increase of \mathbf{f} .

In the MEC-Enabled vehicular cloud system. It is unrealistic not to take into account the mobility of the vehicle, we then investigated the impact of vehicle mobility on system performance. Assume the variation of the vehicles speed is negligible within the reference time interval. In order to further illustrate the influence of speed-induced Doppler shift on system performance, the comparison experiment between the benchmark value and the increasing speed measurement under the condition of constant vehicle speed is simulated in the system.

Since the relative speed in the V-RSU link is zero, And the speed of all vehicles is the same in the same network there is no Doppler effect. Then the vehicle speed on the road is set to 20 m/s, 30 m/s, 40 m/s, 50 m/s and 60 m/s, respectively. It can be seen from Fig. 5 that with the increase of vehicle speed, the utility value of the vehicular network decreases. This is because the higher speed will cause a greater Doppler frequency shift in the network, increase channel uncertainty. The result also proves that methods tend to obtain better utility when the vehicle speed is low.

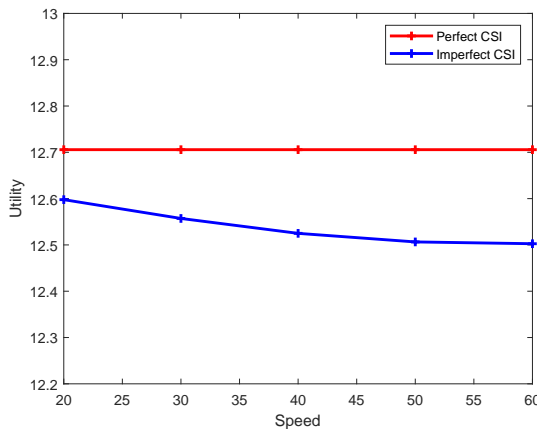


Fig. 5: Comparison of average system utility against different speed.

In order to further verify the performance of the proposed scheme after considering the mobility of the vehicle, the figure.6 describes the effect of the same speed and different speeds of each vehicle under different ε_1 on the total utility,

and it can be seen from the figure that with the change of ε_1 , the system utility also changes, and the utility at different speeds of each vehicle is higher than that of all vehicles at the same speed, which characterizes the high robustness of the proposed method in complex dynamic vehicle networks.

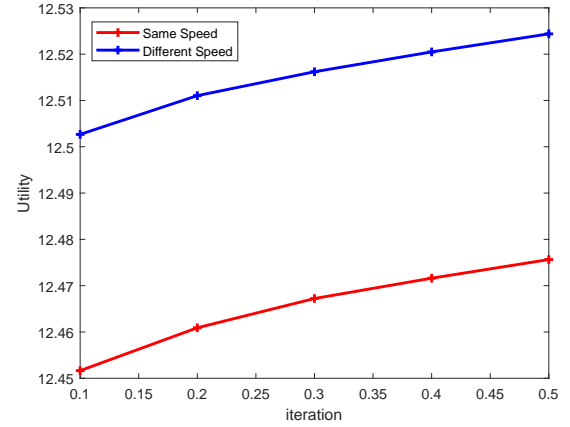


Fig. 6: Comparison of average system utility against different ε_1 .

In terms of computing resources allocation, we choose the default task input size as $d_u = 420KB$ (following [28]), We now evaluate the system utility performance against different benchmark schemes. The purpose of this section is to show the convergence of our proposed algorithm and its performance is better than three benchmark schemes through some simulation results. The benchmark schemes are described as follow

- 1) “Independent Offloading and power control” (denoted as “IOP”): the vehicles independently make power control and the computing resources allocation.
- 2) “Without vehicle power control” (denoted as “Without-VPC”): The transmit power of the vehicles is set as average power during the offloading.
- 3) “Without computing resources allocation”: (denoted as “Without-CRA”), The transmit power of the vehicles is set as average power during the offloading.

Fig. 6 is the iterative convergence of the total utility of the system in different cases, and it can be seen from the figure that the robust joint optimization performance is better than the other three cases. It can be seen that with the increase of the number of iterations, the four methods converge to a stable value, among which the performance of proposed scheme is the best.

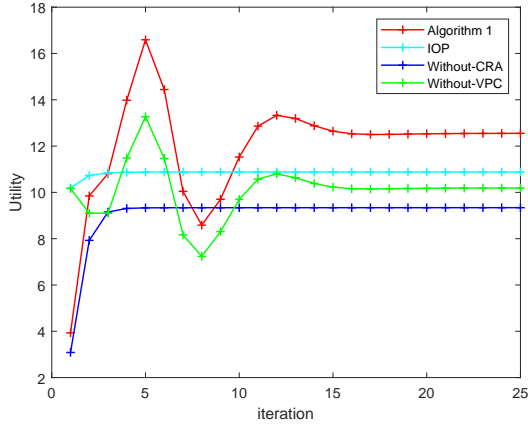


Fig. 7: transmission rate under different numbers.

In order to reflect a more realistic situation, the CPU task load (Megacycles) required for each vehicle are often different, so we set the CPU task load (Megacycles) of the five vehicles to 1600, 1700, 1800, 1900, 2000.

As we can see, with the increase of the ratio of iteration, the average system utility of vehicles changes gradually and tends to be stable. In the independent optimization process, the computing resource allocation is carried out first, and the optimal power allocation is not known at this time, and the power and computing resource alternate optimization method is used, and the corresponding optimal value can be obtained for each iteration. Individual optimization is to first optimize the power \mathbf{p} , and after obtaining the result, the result is used for the optimization of computing resources, and then the computing resources are optimized, and finally, the utility of the system is obtained. However, if joint optimization is used, then both variables can get the optimal value.

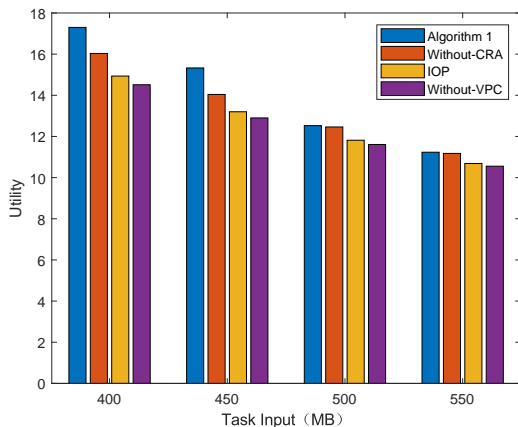


Fig. 8: Comparison of average system utility against different task input size.

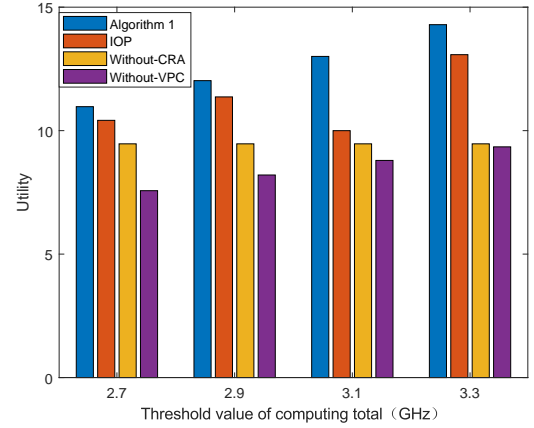
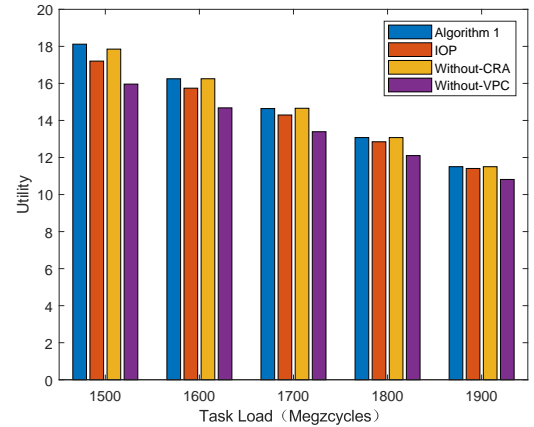
Fig. 9: Comparison of average system utility against different f_{total} .

Fig. 10: Comparison of average system utility against different task workloads.

The average system utility of the four competing schemes are plotted in Fig.8 with different values of d_u . It can be seen that the average system utilities of all schemes decrease with the task input size. Moreover, we observe that the performance gains of the proposed scheme over the other schemes also follow the similar trend. The total system cost comparisons with different f_{total} are shown in Fig.9. Due to the limited computation capability at the cloud, when the computation capability is small, the system utility tend to small. We can clearly see that as the data size increases, the system utility tend to small. This is because when the tasks require more upload time with more data size.

V. CONCLUSION

This paper focuses on the Joint Task Offloading and Resource Allocation for Mobile-Edge Computing Enable Vehicular Networks with channel uncertainty and co-channel interference. The optimization scheme attempt to guarantees vehicles QoS when there exists a maximized utility requirement. Due to the existence of channel uncertainty, the probability forms of interference, delay, and delivery rate constraints are performed.

The underlying optimization problem was formulated as a Mixed-Integer Non-linear Program (MINLP), which is very difficult to solve to optimal, then the SCA technique is applied to transform the non-convex problem of variables coupling into a treatable convex problem. The Task Offloading and power allocation algorithm is developed to achieve practical execution scheme. Simulation results showed that our heuristic algorithm performs closely to the optimal solution and significantly improves the average system offloading utility over traditional approaches.

REFERENCES

- [1] S. Pang, N. Wang, M. Wang, S. Qiao, X. Zhai, and N. N. Xiong, "A Smart Network Resource Management System for High Mobility Edge Computing in 5G Internet of Vehicles," *IEEE Transactions on Network Science and Engineering*, vol. 8, no. 4, pp. 3179–3191, 2021.
- [2] B. Cai, C. Wang, W. ShangGuan, and J. Wang, "Research of information interaction simulation method in Cooperative Vehicle Infrastructure System," in *17th International IEEE Conference on Intelligent Transportation Systems (ITSC)*, 2014, pp. 45–50.
- [3] X.-Q. Pham, T.-D. Nguyen, V. Nguyen, and E.-N. Huh, "Joint Node Selection and Resource Allocation for Task Offloading in Scalable Vehicle-Assisted Multi-Access Edge Computing," *Symmetry*, vol. 11, no. 1, 2019. [Online]. Available: <https://www.mdpi.com/2073-8994/11/1/58>
- [4] Y. Wang, P. Lang, D. Tian, J. Zhou, X. Duan, Y. Cao, and D. Zhao, "A Game-Based Computation Offloading Method in Vehicular Multiaccess Edge Computing Networks," *IEEE Internet of Things Journal*, vol. 7, no. 6, pp. 4987–4996, 2020.
- [5] P. Dai, K. Hu, X. Wu, H. Xing, F. Teng, and Z. Yu, "A Probabilistic Approach for Cooperative Computation Offloading in MEC-Assisted Vehicular Networks," *IEEE Transactions on Intelligent Transportation Systems*, vol. 23, no. 2, pp. 899–911, 2022.
- [6] A. Ahmed, A. Abdul, K. Omprakash, M. J. Usman, O. Syed, and Aanchal, "Mobile Cloud Computing energy-aware Task Offloading (mcc: Eto)," 2016.
- [7] Y.-a. Xie, Z. Liu, K. Y. Chan, and X. Guan, "Energy-Spectral Efficiency Optimization in Vehicular Communications: Joint Clustering and Pricing-Based Robust Power Control Approach," *IEEE Transactions on Vehicular Technology*, vol. 69, no. 11, pp. 13 673–13 685, 2020.
- [8] X. Chen, L. Pu, L. Gao, W. Wu, and D. Wu, "Exploiting Massive D2D Collaboration for Energy-Efficient Mobile Edge Computing," *IEEE Wireless Communications*, vol. 24, no. 4, pp. 64–71, 2017.
- [9] J. Liu, N. Kato, J. Ma, and N. Kadowaki, "Device-to-Device Communication in LTE-Advanced Networks: A Survey," *IEEE Communications Surveys & Tutorials*, vol. 17, no. 4, pp. 1923–1940, 2015.
- [10] H. Zhou, W. Xu, Y. Bi, J. Chen, Q. Yu, and X. S. Shen, "Toward 5G Spectrum Sharing for Immersive-Experience-Driven Vehicular Communications," *IEEE Wireless Communications*, vol. 24, no. 6, pp. 30–37, 2017.
- [11] T. X. Tran and D. Pompili, "Joint Task Offloading and Resource Allocation for Multi-Server Mobile-Edge Computing Networks," *IEEE Transactions on Vehicular Technology*, vol. 68, no. 1, pp. 856–868, 2019.
- [12] Z. Liu, C. Liang, Y. Yuan, K. Y. Chan, and X. Guan, "Resource Allocation Based on User Pairing and Subcarrier Matching for Downlink Non-Orthogonal Multiple Access Networks," *IEEE/CAA Journal of Automatica Sinica*, vol. 8, no. 3, pp. 679–689, 2021.
- [13] L. Liang, G. Y. Li, and W. Xu, "Resource Allocation for D2D-Enabled Vehicular Communications," *IEEE Transactions on Communications*, vol. 65, no. 7, pp. 3186–3197, 2017.
- [14] Y. Ren, F. Liu, Z. Liu, C. Wang, and Y. Ji, "Power Control in D2D-Based Vehicular Communication Networks," *IEEE Transactions on Vehicular Technology*, vol. 64, no. 12, pp. 5547–5562, 2015.
- [15] Y. Chen, Y. Wang, and L. Jiao, "Robust Transmission for Reconfigurable Intelligent Surface Aided Millimeter Wave Vehicular Communications With Statistical CSI," *IEEE Transactions on Wireless Communications*, vol. 21, no. 2, pp. 928–944, 2022.
- [16] S. Wang, W. Shi, and C. Wang, "Energy-Efficient Resource Management in OFDM-Based Cognitive Radio Networks Under Channel Uncertainty," *IEEE Transactions on Communications*, vol. 63, no. 9, pp. 3092–3102, 2015.
- [17] H. Xiao, D. Zhu, and A. T. Chronopoulos, "Power Allocation With Energy Efficiency Optimization in Cellular D2D-Based V2X Communication Network," *IEEE Transactions on Intelligent Transportation Systems*, vol. 21, no. 12, pp. 4947–4957, 2020.
- [18] L. T. Tan and R. Q. Hu, "Mobility-Aware Edge Caching and Computing in Vehicle Networks: A Deep Reinforcement Learning," *IEEE Transactions on Vehicular Technology*, vol. 67, no. 11, pp. 10 190–10 203, 2018.
- [19] A. Nemirovski and A. Shapiro, "Convex Approximations of Chance Constrained Programs," *SIAM Journal on Optimization*, vol. 17, no. 4, pp. 969–996, 2007.
- [20] Y. Cui, L. Du, H. Wang, D. Wu, and R. Wang, "Reinforcement Learning for Joint Optimization of Communication and Computation in Vehicular Networks," *IEEE Transactions on Vehicular Technology*, vol. 70, no. 12, pp. 13 062–13 072, 2021.
- [21] T. Kim, D. J. Love, and B. Clerckx, "Does Frequent Low Resolution Feedback Outperform Infrequent High Resolution Feedback for Multiple Antenna Beamforming Systems?" *IEEE Transactions on Signal Processing*, vol. 59, no. 4, pp. 1654–1669, 2011.
- [22] A. Sakr and E. Hossain, "Cognitive and Energy Harvesting-Based D2D Communication in cellular networks: Stochastic geometry modeling and analysis," *Communications, IEEE Transactions on*, vol. 63, 05 2014.
- [23] L. Yang, J. Cao, H. Cheng, and Y. Ji, "Multi-User Computation Partitioning for Latency Sensitive Mobile Cloud Applications," *IEEE Transactions on Computers*, vol. 64, no. 8, pp. 2253–2266, 2015.
- [24] Z. Liu, J. Su, Y.-a. Xie, K. Ma, Y. Yang, and X. Guan, "Resource Allocation in D2D-Enabled Vehicular Communications: A Robust Stackelberg Game Approach Based on Price-Penalty Mechanism," *IEEE Transactions on Vehicular Technology*, vol. 70, no. 8, pp. 8186–8200, 2021.
- [25] X. Li, L. Ma, Y. Xu, and R. Shankaran, "Resource Allocation for D2D-Based V2X Communication With Imperfect CSI," *IEEE Internet of Things Journal*, vol. 7, no. 4, pp. 3545–3558, 2020.
- [26] D. P. Bertsekas, "Nonlinear Programming: 2nd Edition," 1999.
- [27] Z. Liu, Y. Xie, K. Y. Chan, K. Ma, and X. Guan, "Chance-Constrained Optimization in D2D-Based Vehicular Communication Network," *IEEE Transactions on Vehicular Technology*, vol. 68, no. 5, pp. 5045–5058, 2019.
- [28] X. Chen, L. Jiao, W. Li, and X. Fu, "Efficient multi-user computation offloading for mobile-edge cloud computing," *IEEE/ACM Transactions on Networking*, vol. 24, 10 2015.